Neuro-Oncology

20(10), 1344–1355, 2018 | doi:10.1093/neuonc/noy068 | Advance Access date 30 April 2018

PI3K activation in neural stem cells drives tumorigenesis which can be ameliorated by targeting the cAMP response element binding protein

Paul M. Daniel, Gulay Filiz, Daniel V. Brown, Michael Christie, Paul M. Waring, Yi Zhang, John M. Haynes, Colin Pouton, Dustin Flanagan, Elizabeth Vincan, Terrance G. Johns, Karen Montgomery, Wayne A. Phillips, and Theo Mantamadiotis

Department of Pathology (P.M.D., G.F., D.V.B., M.C., P.M.W., T.M.), Department of Microbiology and Immunology, The University of Melbourne, Parkville, Victoria, Australia (T.M.); Monash Institute of Pharmaceutical Sciences, Monash University, Parkville, Victoria, Australia (Y.Z., J.M.H., C.P.); Molecular Oncology Laboratory, The University of Melbourne, Parkville, Victoria, Australia (D.F., E.V.); Victorian Infectious Diseases Reference Laboratory, Peter Doherty Institute, Melbourne, Victoria, Australia (E.V.); School of Biomedical Sciences, Curtin University, Perth, Western Australia, Australia (E.V.); Oncogenic Signalling Laboratory, Telethon Kids Institute, Subiaco, Western Australia, Australia (T.G.J.); Cancer Biology and Surgical Oncology Research Laboratory, Peter MacCallum Cancer Centre, Melbourne, Victoria, Australia (K.M., W.A.P.); Sir Peter MacCallum Department of Oncology, The University of Melbourne, Melbourne, Victoria, Australia (W.A.P.); Department of Surgery (Royal Melbourne Hospital), The University of Melbourne, Parkville, Victoria, Australia (T.M.)

Corresponding Author: Theo Mantamadiotis, Department of Pathology, Department of Microbiology and Immunology, The University of Melbourne, Parkville, VIC, Australia and Department of Surgery (RMH), The University of Melbourne, Parkville, VIC, Australia (theom@unimelb.edu.au).

Abstract

Background. Hyperactivation of phosphoinositide 3-kinase (PI3K) signaling is common in cancers, but the precise role of the pathway in glioma biology remains to be determined. Some understanding of PI3K signaling mechanisms in brain cancer comes from studies on neural stem/progenitor cells (NSPCs), where signals transmitted via the PI3K pathway cooperate with other intracellular pathways and downstream transcription factors to regulate critical cell functions.

Methods. To investigate the role of the PI3K pathway in glioma initiation and development, we generated a mouse model targeting the inducible expression of a PIK3CA^{H1047A} oncogenic mutant and deletion of the PI3K negative regulator, phosphatase and tensin homolog (PTEN), to NSPCs.

Results. Expression of a Pik3ca^{H1047A} was sufficient to generate tumors with oligodendroglial features, but simultaneous loss of PTEN was required for the development of invasive, high-grade glioma. Pik3ca^{H1047A}–PTEN mutant NSPCs exhibited enhanced neurosphere formation which correlated with increased Wnt signaling, while loss of cAMP response element binding protein (CREB) in Pik3ca^{H1047A}–Pten mutant tumors led to longer symptom-free survival in mice.

Conclusion. Taken together, our findings present a novel mouse model for glioma demonstrating that the PI3K pathway is important for initiation of tumorigenesis and that disruption of downstream CREB signaling attenuates tumor expansion.

Keywords

CREB | mouse model | neural stem cells | PIK3CA | PTEN

Importance of the study

This study demonstrates that PI3K mutations in NSPCs can initiate glioma-like tumors. Mutant NSPCs exhibited increased PI3K signaling but also showed enhanced CREB transcription factor activation, which promotes cell proliferation, as well as enhanced Wnt signaling, which promotes self-renewal. Tumors were switched to a less malignant state by simultaneous deletion of CREB, raising the possibility that CREB may be an important anticancer drug target.

Genetically engineered mouse models have demonstrated that various genes can initiate glioma development, with the first models expressing constitutively activated mutant growth factor receptors, including epidermal growth factor receptor (EGFR), or mutated signaling molecules, including Ras and Akt.[1,2] Genes enabling the initiation of high-grade gliomas (HGGs) include combinations of *NF1, TP53, PTEN, Akt, Ras*, and *INK4a/ARF*.[3–6] Models targeting glial cells,[1,4,7] oligodendrocyte precursor cells, astrocytes, or neurons also initiate HGG.[8,9] The role of brain tumor stem cells (BTSCs) has been demonstrated by targeting genetic mutations/deletions in neural stem/progenitor cells (NSPCs),[2,3,5,6,9–11] highlighted by a study demonstrating that ablation of BTSCs inhibits tumor growth.[12]

The signaling pathways driving HGG overlap with those activated in other cancers and involve complex interactions between oncogenes and tumor suppressors, many of which regulate the phosphoinositide 3-kinase (PI3K) and mitogen-activated protein kinase (MAPK) pathways. These pathways trigger a cascade of downstream kinases leading to the activation of transcription factors, including the cAMP response element binding protein (CREB), which is upregulated in glioblastoma (GBM) and has a role in NSPC and GBM cell proliferation.[13,14] Emerging evidence suggests that oncogenic PI3K and MAPK signals converge with Wnt signaling to regulate cancer cell growth and proliferation[15] and that in GBM, Wnt signaling has a role in cancer stem cell maintenance.[16]

When one considers the upstream components of the PI3K pathway, including EGFR, the PI3K catalytic and regulatory subunits, as well as the pathway's major negative regulator, phosphatase and tensin homolog (PTEN), 63% of HGGs exhibit an alteration in at least one of these genes.[17] A major catalytic subunit of PI3K, encoded by the phosphatidylinositol-4,5-bisphosphate 3-kinase catalytic subunit alpha gene (*PIK3CA*), is among the 3 top oncogenic drivers in GBM; the other drivers are *EGFR* and *TP53*.[18] Indeed, *PIK3CA* mutations are reported in up to 17% of low- and high-grade pediatric and adult brain cancers, with higher-grade and treatment-resistant tumors exhibiting higher mutation rates.[17,19] Full activation of the PI3K pathway not only requires enhanced catalytic activity to drive key downstream kinases such as Akt but also requires the inactivation of the phosphatase activity of PTEN.[20,21] Deletion of PTEN in NSPCs leads to enhanced proliferative activity in the stem cell niche but no tumor development.[22,23] *Pten* deletion in combination with *p53* and/or *Rb1* loss results in the development of astrocytic high-grade tumors.[4] However, the effects of pro-oncogenic mutations involving the PI3K catalytic (p110α) and regulatory (p85) subunits have not been investigated.

To better understand the role of the PI3K pathway, we targeted the PI3K pathway in mouse NSPCs by conditional activation of an oncogenic mutation in *Pik3ca*, the gene encoding the PI3K p110α catalytic subunit,[24] in combination with PTEN deletion and show that these mutations are sufficient to initiate tumor growth. To investigate the downstream transcriptional programs regulated by the PI3K pathway, we deleted CREB and show that CREB loss slows tumor growth and leads to a less aggressive phenotype.

Materials and Methods

Ethics Statement

Mouse experiments were carried out with the approval of The University of Melbourne, School of Biomedical Sciences (AEC No 1112336.1) and Peter MacCallum Cancer Center (AEEC No. E406) Animal Ethics Committees.

Mouse Breeding

Mice heterozygous for a latent Cre recombinase (Cre)-inducible knock-in of the $Pik3ca^{H1047R}$ mutation ($Pik3ca^{H1047R\text{-}lox}$)[24] and/or 2 Cre-inducible *Pten* deletion alleles ($Pten^{loxP/loxP}$)[23] were crossed with mice expressing a single (heterozygous) *Nestin-CreER*^{T2} transgene.[25] Further F1 crosses generated mice which were heterozygous for mutant $Pik3ca^{H1047R}$ ($Pik3ca^{H1047R\text{-}lox}$–*Nestin-CreER*^{T2}) and homozygous *Pten* deletion ($Pten^{loxP/loxP}$–*Nestin-CreER*^{T2}) ($Pten^{\Delta}$). Mice were housed and genotyped as previously described.[24,26] See Supplementary Methods for details.

In Vivo Tumor Induction

Control ($Pik3ca^{H1047R\text{-}lox}$–$Pten^{lox/lox}$), double mutant ($Pik3ca^{H1047R\text{-}lox}$–$Pten^{lox/lox}$–*Nestin-CreER*^{T2}), or triple mutant ($Pik3ca^{H1047R\text{-}lox}$–$Pten^{lox/lox}$–$Creb^{lox/lox}$–*Nestin-CreER*^{T2}) mice were treated with tamoxifen at either 1 day or 6–8 weeks of age, as described previously.[27]

Histology and protein analysis

Brain tissue was fixed by intracardiac perfusion with 4% paraformaldehyde, and immunohistochemistry was performed as described previously.[26] For western blotting, cells were lysed in radioimmunoprecipitation assay buffer. Antibodies are detailed in the Supplementary Methods.

NSPC Culture

Refer to the Supplementary Methods for isolation of NSPC protocol. For experiments involving NSPCs, mutant NSPCs were generated by transient (24 h) treatment with 0.02 mg/mL 4-hydroxy-tamoxifen (4-OHT) in ethanol to induce Cre-mediated recombination of *floxed* alleles, while control cells were derived from the same genotype but treated with vehicle only (ethanol). 4-OHT was removed after 24 h and never included in the medium in further experiments.

Cell Cycle Analysis

Cells in phosphate buffered saline (PBS) were fixed in cold 100% ethanol. Cells were washed 3 times with PBS and incubated with 4′,6′-diamidino-2-phenylindole (DAPI) (5 μg/mL; Thermo Fisher Scientific) for 15 min on ice. Cells were then washed, suspended in PBS, and analyzed by fluorescence activated cell sorting (LSR Fortessa 405 nm). Cells were gated with forward scatter width versus DAPI (405 nm) to exclude doublets and debris. A histogram of DAPI versus count was generated and analyzed using FlowLogic v6 software to identify the population (%) of cells in each of the cell cycle phases.

Proliferation Assays

Resazurin solution (Sigma) was diluted in media and added to wells, in 96-well plates, to obtain a 10% v/v solution before incubation for 3 h at 37°C. Plates were analyzed using the EnSpire Plate Reader (PerkinElmer).

Migration Assay

Single neurospheres in Dulbecco's modified Eagle's medium F12 with growth factors and supplements (see NSPC Culture method, above) were placed into a 96-well plate (1 sphere/well) for 48 h and assayed using theTrevigen 96-well 3D spheroid basement membrane extracts cell invasion assay kit (Bio Scientific). Neurospheres were incubated either with (test) or without (control) addition of invasion matrix for 48 h. Spheres were photographed and invasion area was calculated by measuring the area of spread and subtracting the control neurosphere invasion area using ImageJ (http://rsb.info.nih.gov/ij/index.html).

Extreme Limiting Dilution Analysis

Neurospheres were dissociated and plated in suspension media at 20, 10, 5, and 1 cell per well with 24 replicates per cell density. Wells were photographed after 7 days and the number of wells with one or more spheres greater than ~20 μm diameter was scored. Data were analyzed using online analysis[28] (http://bioinf.wehi.edu.au/software/elda/).

Statistical analysis

Student's *t*-test was used and results presented as mean ± SD or SEM, as indicated in relevant sections. $P < 0.05$ (*) was considered significant.

Results

Activation of *Pik3ca*^{H1047R} Expression in NSPCs Is Sufficient for Tumor Initiation but Simultaneous Deletion of *Pten* Is Necessary for the Development of Invasive Tumors

The data from all mice analyzed are summarized in Table 1. Control *Pik3ca*$^{H1047R\text{-}lox}$–*Pten*$^{loxP/loxP}$ mice without the *Nestin-CreER*^{T2} transgene but treated with tamoxifen did not develop neurological symptoms or show evidence of tumor growth over the experimental time window of >200 days (Fig. 1). Single mutant *Pten*$^{\Delta}$ mice showed no overt abnormalities but did exhibit increased subventricular zone (SVZ) cellularity and proliferation compared with

Table 1 Mice used in this study and the treatment and outcome of the analysis

Mutation(s)*	Tamoxifen Treated Mice	Tamoxifen at Age (days)	Endpoint Post-tamoxifen (days)	Tumors	Histopathology
Pik3ca^{H1047R}–*nesCre*	7	42–56	>222	Yes (100% from 4 examined)	Low grade, oligodendroglioma
Pten$^{\Delta}$–*nesCre*	3	42–56	>214	No (3 examined)	—
Pik3ca^{H1047R}–*Pten*$^{\Delta}$–*nesCre*	30	42–56	55 to 90	Yes (100% from 20 examined)	High-grade glioma
Pik3ca^{H1047R}–*Pten*$^{\Delta}$–*nesCre*	3	1	28 to 43	Yes (100% from 3 examined)	High-grade glioma
**Pik3ca*^{H1047R}–*Pten*$^{\Delta}$–*nesCre*	0	—	>200	No (2 examined)	—
Pik3ca^{H1047R}–*Pten*$^{\Delta}$–*CREB*$^{\Delta}$–*nesCre*	14	42–56	71 to >167	Yes (100% from 6 examined)	Glioma with large cells
**Pik3ca*^{H1047R}–*Pten*$^{\Delta}$	2	42–56	>214	No (2 examined)	—

**Pik3ca*^{H1047R}–*Pten*$^{\Delta}$ mice without the Cre transgene which were treated with tamoxifen or *Pik3ca*^{H1047R}–*Pten*$^{\Delta}$–nesCre mice not tamoxifen treated showed no signs of disease or neurological symptoms, nor evidence of brain tumors.

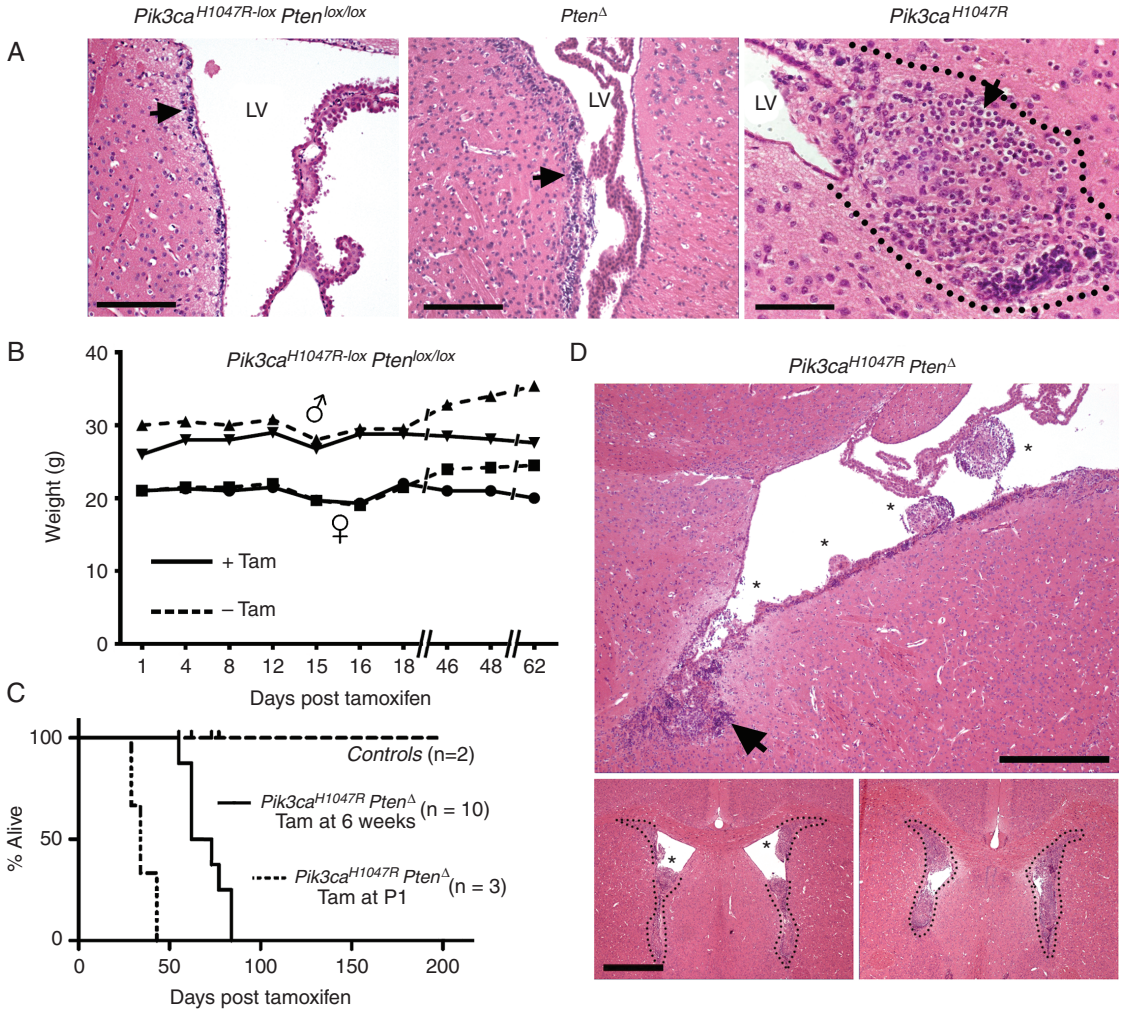

Fig. 1 *Pik3ca*^{H1047R} tumors exhibit oligodendroglial features while combined *Pik3ca*^{H1047R} expression and *Pten-deleted* tumors exhibit extensive growth. (A) Hematoxylin and eosin (HE) staining of brains from wild-type control mice (tamoxifen-treated *Pik3ca*^{H1047R}–*Pten*$^{lox/lox}$ without *Nestin-CreER*^{T2}) showing the SVZ layer (arrow) harboring NSPCs. Single mutant homozygous *Pten*$^{\Delta}$ mice showed thickening of the SVZ layer (arrow). Single mutant heterozygous *Pik3ca*^{H1047R} tumor (all brains were dissected at 181 days post-tamoxifen), within the dotted outline, showing cells with characteristic perinuclear halos (arrow). Scale bar is 250 μm for the 2 left images and 100 μm for *Pik3ca*^{H1047R}. (B) Body weight of a representative adult mouse (6 wk of age) which received tamoxifen (Tam) at day 0. (C) Kaplan–Meier survival analysis shows that only tamoxifen-treated double mutant *Pik3ca*^{H1047R}–*Pten*$^{\Delta}$ adult (n = 10) and newborn (P1) mouse (n = 3) cohorts compared with WT controls (n = 12). (D) HE staining of a double mutant *Pik3ca*^{H1047R}–*Pten*$^{\Delta}$ brain (all brains were dissected at 55 or 62 days post-tamoxifen) show multiple tumors (*) growing out from the neurogenic zone (arrows) into the lateral ventricles (LV) (upper panel). Scale bar is 200 μm. Anterior brain sections (lower panels) demonstrate almost complete occlusion of the ventricular space by the tumor tissue. Scale bar is 1 mm.

controls (Fig. 1A), as reported previously.[23] Examination of single mutant *Pik3ca*^{H1047R} mouse brains between 42 and 222 days post tamoxifen administration revealed the presence of tumors in/adjacent to the lateral ventricles (LVs) (Fig. 1A). Tumors from 4 *Pik3ca*^{H1047R} mice exhibited numerous cells with perinuclear halos or "fried egg" cells with oligodendrocyte transcription factor (Olig2) expression; features associated with oligodendroglioma (Fig. 1A and Supplementary Figure S1).

Tamoxifen treatment of *Pik3ca*$^{H1047R\text{-}lox}$–*Pten*$^{loxP/loxP}$–*Nestin-CreER*^{T2} (referred to as *Pik3ca*^{H1047R}–*Pten*$^{\Delta}$) 6- to 8-week-old mice resulted in a completely penetrant (100%; 30/30 mice) neurological phenotype 55–90 days after tamoxifen administration. An early sign of ill health was a decline in body weight (Fig. 1B), followed by the appearance of progressively more severe neurological symptoms. The first neurological manifestation was ataxia, followed by sporadic seizures and a gradual increase in seizure frequency and length. The experimental endpoint was when weight loss was more than 15% of the start weight and/or when seizures occurred more than 3 times per day, and when a seizure lasted more than 1 min. Double mutant

mice reached the experimental endpoint between 55 and 90 days (Fig. 1C). Single mutant *Pik3ca*^{H1047R} expression or *Pten* mice showed no symptoms or reduced survival over 200 days (Fig. 1B, C and Table 1). When *Pik3ca*^{H1047R}–*Pten*$^{\Delta}$ mutations were activated in 1-day-old newborn mice (P1) via tamoxifen treatment of the mother and transmission of the tamoxifen to pups via the mother's milk, the pups began exhibiting severe neurological symptoms between 28 and 43 days (Fig. 1C); faster than in adult mice treated with tamoxifen but with morphologically similar tumors to adult mice.

Adult *Pik3ca*^{H1047R}–*Pten*$^{\Delta}$ brains exhibited hypercellularity of the SVZ, with multiple tumor nodules protruding into the LV (Fig. 1D, upper panel) and tumors filling the anterior LV (Fig. 1D lower panels). Hypercellular clusters were present along the SVZ with tumor cell migration into tumor nodules (Fig. 2A, B). Tumor cells invaded the brain parenchyma and white matter tracts, including the corpus callosum (Fig. 2C). Apoptotic cells and mitoses were present, lying among atypical, irregularly arranged tumor cells and blood vessels (Fig. 2D and Supplementary Figure S2A). Rosette-like cell arrangements were noted in one tumor (Supplementary Figure S2B).

Pik3ca^{H1047R}–*Pten*$^{\Delta}$ tumors expressed glial fibrillary acidic protein (GFAP) (Fig. 2E) and β-III-tubulin (Tuj1) (Fig. 2F): evidence of glial and neuronal differentiation. Phosphorylated (p)Akt and pRps6 were expressed in tumor cells (Fig. 2G), demonstrating PI3K pathway activation. Activation of phospho–extracellular signal-regulated kinase (ERK)1/2 (pERK1/2 [pMAPK]) and phospho-CREB (pCREB) expression showed that other oncogenic signaling and transcriptional pathways were coactivated (Fig. 2G). Ki67 and nestin expression demonstrated that tumors also harbored proliferating, immature cells, with some Olig2-positive cells observed (Supplementary Figure S3). Overall, *Pik3ca*^{H1047R}–*Pten*$^{\Delta}$ tumors exhibited heterogeneous features, consistent with high-grade (grade III) astrocytic tumors.

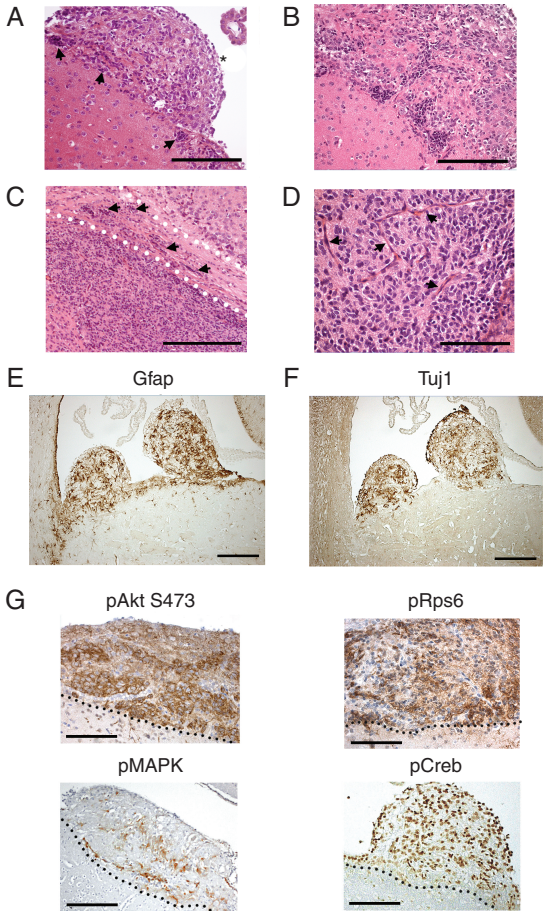

Fig. 2 Mutant *Pik3ca*^{H1047R}–*Pten*$^{\Delta}$ NSPC initiated tumors exhibit features consistent with malignant glioma. (A) A prominent tumor nodule (*) and hyperplastic germinal zones (arrows) (A, B). Tumor cell invasion (arrows) into the brain parenchyma and corpus callosum (demarcated by the dotted lines) (C); (D) tumor vascularization (arrows). Expression of astrocytoma markers GFAP (E) and Tuj1 (F). (G) Elevated expression of pAkt(Ser473), pRpS6, pMAPK (pERK1/2), and pCREB. The dotted lines represent the SVZ–tumor interface, with tumors lying above the dotted line. Scale bars are: 200 μm for (A), (E), (F); 100 μm for (B); 500 μm for (C); 20 μm for (D) (all brains were dissected at 55 or 62 days post-tamoxifen).

Mutant NSPCs Exhibit Enhanced PI3K Signaling and Subtle Shift in Cell Cycle

To investigate the cellular characteristics of mutant cells, NSPCs were isolated from the SVZ of 4-week-old mice carrying the *Nestin-Cre* transgene and latent *Pik3ca*^{H1047R}, *Pten*$^{lox/lox}$, and double mutant *Pik3ca*^{H1047R}–*Pten*$^{lox/lox}$ alleles. NSPCs were propagated as neurospheres, and mutations were activated using 4-OHT. Comparison of PI3K pathway activation by expression analysis of pAkt(Ser473) in wild type (WT), *Pik3ca*^{H1047R}–*Pten*$^{\Delta}$, *Pik3ca*^{H1047R}, and *Pten*$^{\Delta}$ NSPCs showed that PI3K activation was strongest in double mutant *Pik3ca*^{H1047R}–*Pten*$^{\Delta}$ NSPCs (Supplementary Figure S4). Short-term proliferation assays revealed no significant differences between genotypes. Cell cycle phase analysis revealed subtle differences in S-phase, where *Pik3ca*^{H1047R}–*Pten*$^{\Delta}$ and *Pten*$^{\Delta}$ NSPCs showed more cells in S-phase (DNA-replication phase) than both *Pik3ca*^{H1047R} and WT control cells (Supplementary Figure S5).

Incomplete Recombination Directed by the Nestin-Cre^{ERT2} Transgene

PCR analysis of the *Pten* allele in NSPCs carrying the *loxP* alleles and the *Nestin-Cre*^{ERT2} transgene to determine DNA recombination efficiency following 4-OHT treatment showed that NSPC cultures harbored a mixture of mutant and nonmutant cells (Supplementary Figure S6), irrespective of the presence or absence of further *floxed* alleles. Given reports showing that *Nestin* promoters may drive inefficient Cre-mediated recombination of some floxed alleles in NSPCs,[29] we surmised that the *Nestin-Cre*^{ERT2} transgene led to incomplete recombination of the *Pten*$^{lox/lox}$ allele in 4-OHT treated cells. In vivo, mosaic expression of the oncogenic mutations is sufficient for tumor initiation,

since even a small population of mutant founder/initiating tumor cells can proliferate to give rise to the larger tumor mass and disease. Considering this, further in vitro experiments were performed using NSPCs derived from the SVZ of *Pik3ca^{H1047R}–Pten$^{lox/lox}$–UBC-Cre^{ERT2}* mice generated previously,[30] where Cre^{ERT2} expression under the control of the *Ubiquitin* promoter results in complete recombination in all cells exposed to 4-OHT, demonstrated by PCR (Supplementary Figure S6) and loss of PTEN protein (Supplementary Figure S7).

Pik3ca^{H1047R}–Pten$^{\Delta}$ Mutant NSPCs Exhibit Abnormal Morphology and Enhanced Migration

Pik3ca^{H1047R}–Pten$^{\Delta}$ neurospheres formed loosely aggregated rough-edged spheres (Fig. 3A) compared with parental WT neurospheres. Moreover, mutant NSPCs had more filopodia compared with controls (Fig. 3A, B), a feature associated with a more invasive, malignant phenotype in GBM.[31] Incorporation of the thymidine analog, 5-ethynyl-2′-deoxyuridine (EdU) and flow cytometry analysis showed that *Pik3ca^{H1047R}–Pten$^{\Delta}$* cells had a higher proliferation rate compared with WT cells (Fig. 3C). Mutant cells showed enhanced pAkt expression and increased expression of cyclins B1 and D1 (Fig. 3D).

Seeding single neurospheres into a gel matrix showed that *Pik3ca^{H1047R}–Pten$^{\Delta}$* NSPCs migrated to cover more than 3 times the area compared with WT NSPCs (Fig. 3E, F), demonstrating increased migratory capacity. Moreover, seeding cells at high density for 72 h showed that mutant NSPCs detached and migrated away from spheres, unlike control NSPCs at the same density (Supplementary Figure S8).

Enhanced Sphere-Forming Capacity, Persistent Nestin Expression, and Wnt Pathway Activation in *Pik3ca^{H1047R}–Pten$^{\Delta}$* Mutant NSPCs

To determine the long-term proliferation differences between mutant and control NSPCs, cumulative growth was measured over 8 passages (8 wk). *Pik3ca^{H1047R}–Pten$^{\Delta}$* cells showed significantly higher cell numbers from week 2 onward and almost 4 times more cells by 8 weeks (Fig. 4A). To investigate this difference, we examined the neurosphere-forming efficiency of NSPCs using extreme limiting dilution analysis (ELDA).[28] *Pik3ca^{H1047R}–Pten$^{\Delta}$* cells (1 neurosphere forming unit [NSFU])/1.55 cells seeded) formed spheres more efficiently than control cells (1 NSFU/2.01 cells seeded) (Fig. 4B). To test the neurosphere-forming stability of the NSPCs, we subjected the cells to alternating rounds of growth in neurosphere medium, serum-containing medium (to differentiate the cells), and a return to neurosphere medium (Fig. 4C). Flow cytometry analysis demonstrated that the immature marker, nestin, was still expressed in 70% of *Pik3ca^{H1047R}, Pten$^{\Delta}$* differentiated cells, compared with 52% of WT after 7 days (Fig. 4D). Returning differentiated cells to serum-free neurosphere conditions revealed a significantly higher sphere-forming capacity in mutant cells (1 NSFU/15.4 cells seeded) compared with control cells (1 NSFU/36.0 cells seeded) (Fig. 4E). Independent assessment of immature and differentiation markers using nestin+, GFAP+, and Tuj1+ cells grown on laminin for 5 days showed enhanced nestin+ cell stability in mutant NSPCs, under differentiating conditions (Supplementary Fig. S9).

Phosphoprotein measurement showed an upregulation of phosphorylation of various PI3K/Akt pathway–associated factors in mutant NSPCs compared with WT cells (Fig. 5A). To investigate the biological basis of the enhanced neurosphere-forming capacity in *Pik3ca^{H1047R}–Pten$^{\Delta}$* NSPCs, we postulated that Wnt signaling was upregulated in mutant cells, due to the increase in glycogen synthase kinase 3 (GSK3)β phosphorylation and Wnt signaling. Analysis of NSPCs showed that β-catenin was expressed at higher levels in mutant nuclei compared with WT cells (Fig. 5B), indicating activation of Wnt signaling. Messenger RNA expression of Wnt pathway stem-cell factors and targets was higher in mutant NSPCs compared with controls (Fig. 5C). CHIR99021 ("CHIR"), a GSK3 inhibitor and Wnt pathway activator, increased neurosphere-forming potential of mutant NSPCs, which was 1:1 (spheres formed per cells seeded) for CHIR-treated NSPCs compared with 1:2.6 for vehicle-treated cells (Fig. 5D). Upstream inhibition of the Wnt pathway using IWP-2 (inhibitor of Wnt processing) did not affect sphere-forming capacity compared with vehicle-treated mutant NSPCs.

Creb1 Deletion Ameliorates Malignancy of *Pik3ca^{H1047R}–Pten$^{\Delta}$* Tumors

Pik3ca^{H1047R}–Pten$^{\Delta}$ tumors expressed high levels of pCREB (Fig. 2G), and this expression overlapped with nestin and GFAP expressing SVZ cells (Fig. 6A). We previously showed that mouse SVZ cells and human glioma express high levels of activated CREB (pCREB).[14,32] To determine the contribution of CREB in brain tumor growth, we used *Creb$^{lox/lox}$* mice[26] to generate triple mutant *Pik3ca$^{H1047R\text{-}lox}$–Pten$^{lox/lox}$–Creb$^{lox/lox}$–Nestin-CreER^{T2}* mice, resulting in deletion of CREB, in addition to the *Pik3ca* and *Pten* mutations to generate *Pik3ca^{H1047R}–Pten$^{\Delta}$-Creb$^{\Delta}$* mice.

CREB-deleted brain tumors exhibited the presence of large cells (Fig. 6B and Supplementary Figure S10) with little or no invasion into nontumor brain parenchyma (Supplementary Figure S10A). CREB-deleted tumors showed a reduction in cell density compared with double mutant tumors (Figure 6B, C and Supplementary Figure S10), with 65% of the cell density of *Pik3ca^{H1047R}–Pten$^{\Delta}$* tumors. Moreover, CREB mutant mice were symptom free for longer (median 125 days) compared with double mutant *Pik3ca^{H1047R}–Pten$^{\Delta}$* mice (median 70 days) (Fig. 6D).

NSPCs were isolated from *Pik3ca$^{H1047R\text{-}lox}$–Pten$^{lox/lox}$–Creb$^{lox/lox}$–Nestin-CreER^{T2}* mice and treated with 4-OHT, which led to efficient recombination of the *Creb$^{lox/lox}$* allele (Supplementary Figure S6), unlike the *Pten$^{lox/lox}$* allele. Assays showed that proliferation was reduced in CREB-deleted NSPCs compared with *Pik3ca^{H1047R}–Pten$^{\Delta}$* cells (Supplementary Figure S11B). Cell cycle analysis showed that CREB mutant NSPCs had fewer (5.9%) S-phase cells and more (80.2%) G0/G1 phase cells compared with

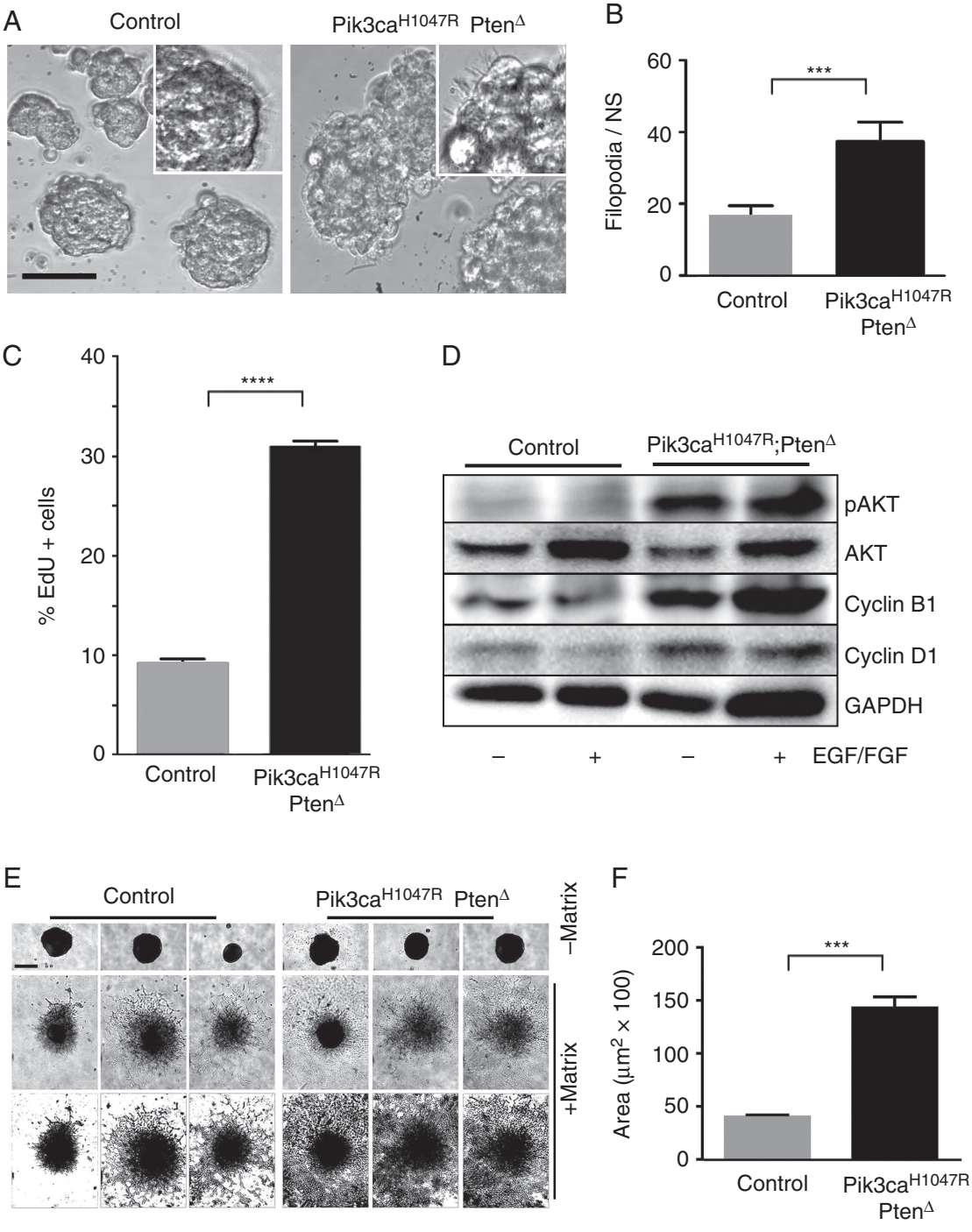

Fig. 3 *Pik3ca^{H1047R}-Pten$^{\Delta}$* mutations enhance the growth and migratory capacity of NSPCs. (A) WT neurospheres exhibit smooth circumscribed borders, while mutant *Pik3ca^{H1047R}–Pten$^{\Delta}$* mutant neurospheres exhibit irregular edges. The inset, above right, highlights part of a neurosphere with filopodia. Scale bar for the main images is 20 μm. (B) The number of filopodia per cell is higher in mutant neurospheres (mean ± SD, $n = 5$; ***$P < 0.001$, Student's *t*-test). (C) *Pik3ca^{H1047R}–Pten$^{\Delta}$* NSPCs exhibited enhanced proliferation, measured by EdU incorporation over 24 h. ****$P < 0.00001$. (D) Western blot shows that *Pik3ca^{H1047R}–Pten$^{\Delta}$* NSPCs express increased pAkt, cyclin B1, and cyclin D1, with or without EGF and basic fibroblast growth factor in the neurosphere medium. (E) Mutant NSPCs exhibit a higher migratory capacity compared with control NSPCs. The lower panels are "threshold" converted images (of the central [+ matrix] images) to enhance the contrast to show the extent of cell migration. Scale bar on top left panel of (c) is 50 μm and applies to all images in the panel. (F) Quantitation of migration is expressed as area of spread (mean ± SD, $n = 5$; ***$P < 0.001$, Student's *t*-test).

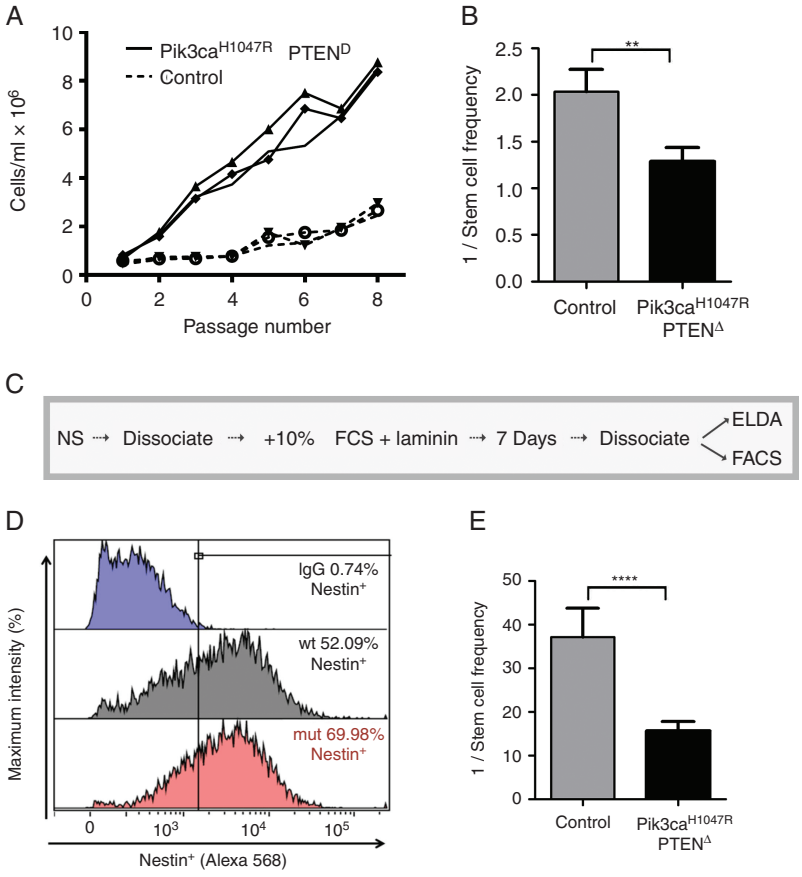

Fig. 4 *Pik3ca^{H1047R}–Pten$^{\Delta}$* mutant NSPCs exhibit enhanced and stable sphere-forming potential under conditions promoting differentiation. (A) Cumulative cell number of control and *Pik3ca^{H1047R}–Pten$^{\Delta}$* NSPCs over 8 passages (1000 cells/mL seeded/1 passage/7 days). Cell counts were performed in triplicate from separate wells. (B) NSPCs seeded at low densities showed a selective advantage in forming a neurosphere compared with control cells; $n = 3$, Student's *t*-test, $^{**}P < 0.01$. (C) The protocol used to test the maintenance of nestin expression and neurosphere-forming capacity following differentiation. (D) Nestin expression by flow cytometry after differentiation for 7 days. (E) Sphere-forming efficiency determined by extreme limiting dilution analysis (ELDA) after cells were returned to neurosphere medium; $n = 3$, $^{****}P < 0.0001$. See Materials and Methods for details.

Pik3ca^{H1047R}–Pten$^{\Delta}$ (12.8% S phase; 70% G0/G1 phase) NSPCs (Supplementary Figure S11C). Sphere-forming capacity of *Creb$^{\Delta}$* NSPCs did not differ compared with *Pik3ca^{H1047R}–Pten$^{\Delta}$* NSPCs (not shown).

Discussion

To our knowledge, no studies have demonstrated a direct involvement of PI3K subunit mutations in glioma in vivo. Large-scale sequencing data suggest that PIK3CA is a key driver of malignant astrocytic brain cancer.[18] Our study demonstrates that expression of constitutive active Pik3ca^{H1047R} can initiate slow-growing oligodendroglial-like tumors when targeted to NSPCs. In patients, *PIK3CA^{H1047R}* mutations are seen in both low- and high-grade gliomas, including anaplastic oligodendroglioma and glioblastoma.[17,19] Homozygous loss of *Pten* led to increased SVZ cellularity but not tumor development, similar to the phenotype previously reported using *Pten$^{lox/lox}$–Nestin-Cre* mice.[23,33] Coexistent mutation of both PIK3CA and deletion of PTEN is rare in glioma patients but the combined genetic aberrations are not absolutely redundant.[34] Inactivation of PTEN and constitutive activation of PIK3CA, which led to maximal PI3K pathway activation (Fig. 3D),[35] is presumably required to drive tumorigenesis, highlighting the importance of cooperative cancer-driving mutations which lead to robust PI3K pathway activation. Further, the Pik3ca mutation only affects p110α, while PTEN will affect both the p110α and other p110 subunits, including p110β, which has a role in glioma cell function,[36,37] further enhancing PI3K signaling.

Pik3ca^{H1047R}–Pten$^{\Delta}$ NSPCs exhibited enhanced migratory properties and sphere-forming stem cell–associated characteristics, consistent with previous studies demonstrating that PI3K pathway activation promotes GBM cell migration,[38] neurosphere formation, and tumorigenicity of glioma stem cells.[39] *Pik3ca^{H1047R}–Pten$^{\Delta}$* NSPCs maintained nestin expression and sphere-forming capacity even after

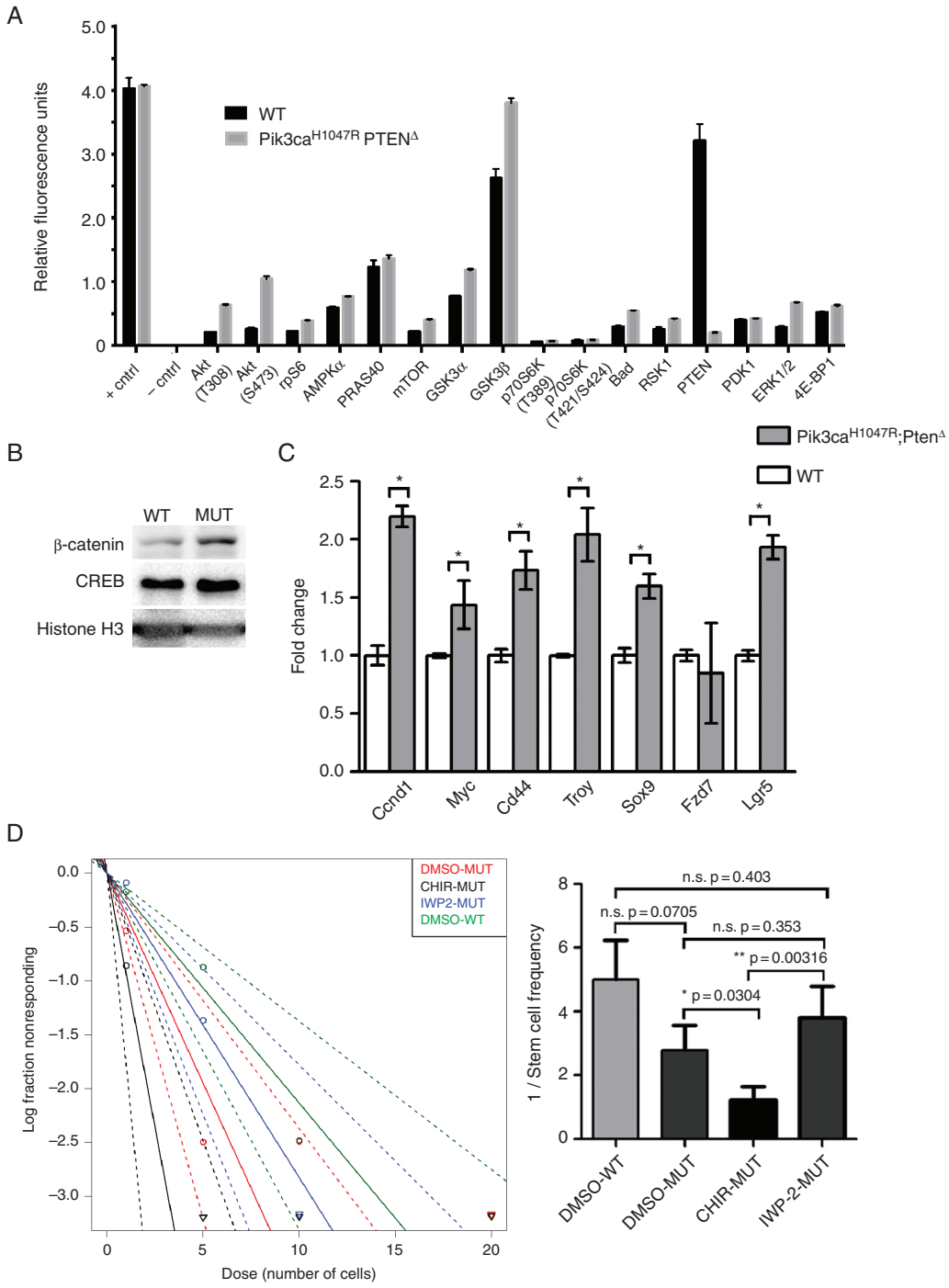

Fig. 5 *Pik3ca^{H1047R}–Pten$^{\Delta}$* mutant NSPCs exhibit enhanced PI3K downstream activity, MAPK activation, Wnt pathway activation, and Wnt pathway–dependent self-renewal capacity. (A) A PathScan Akt Signaling Antibody Array showing the phosphoprotein expression levels of PI3K/Akt-dependent factors in lysates from *Pik3ca^{H1047R}–Pten$^{\Delta}$* mutant and WT NSPCs. (B) Western blot showing increased nuclear β-catenin expression in *Pik3ca^{H1047R}–Pten$^{\Delta}$* mutant NSPCs. Nuclear proteins, CREB, and histone-H3 were used as loading controls (C) Quantitative real-time PCR analysis of Wnt pathway factors showing upregulation of the Wnt signaling in *Pik3ca^{H1047R}–Pten$^{\Delta}$* mutant cells. (D) Extreme limiting dilution analysis of NSPCs showing that Wnt pathway activation by pharmacological inhibition of GSK3β using CHIR99021 (2 μM) increases neurosphere-forming capacity of mutant NSPCs, while Wnt inhibition using IWP-2 (5 μM) reduces neurosphere forming capacity to WT control levels. All error bars are SEM from $n = 3$. *$P < 0.05$ or as indicated in Fig. 5D.

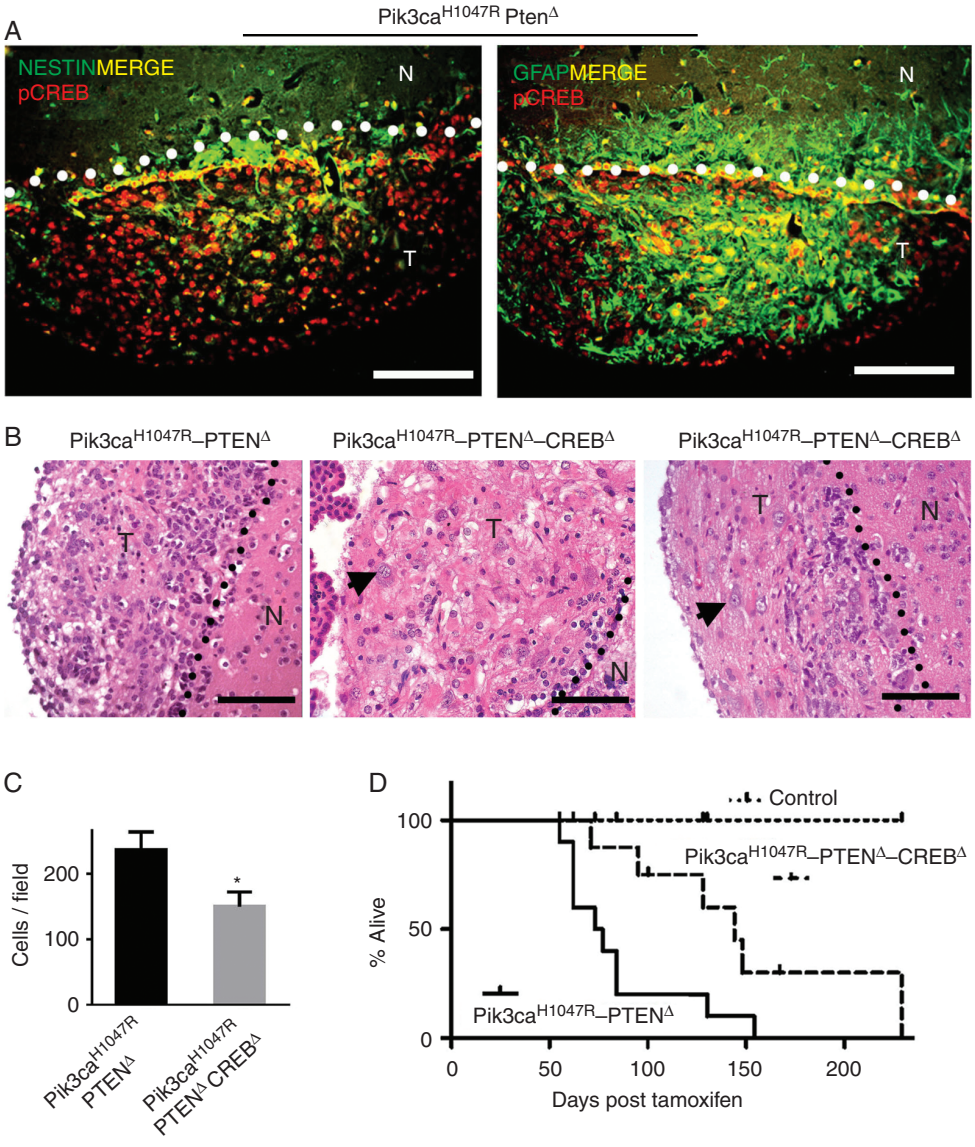

Fig. 6 *Creb* deletion in *Pik3ca^{H1047R}–Pten$^{\Delta}$* NSPCs increases survival by slowing tumor growth. (A) Immunofluorescence analysis of *Pik3ca^{H1047R}–Pten$^{\Delta}$* tumors for expression of pCREB, the neural stem cell marker, nestin, and glial marker, GFAP. The SVZ–tumor boundary is demarcated by the dotted lines, with tumors lying below the line. Scale bars = 100 µm. (B) Hematoxylin and eosin staining showing cellularity differences in tumors derived from double mutant (*Pik3ca^{H1047R}–Pten$^{\Delta}$*) (DM) and triple mutant (*Pik3ca^{H1047R}–Pten$^{\Delta}$–Creb$^{\Delta}$*) mice. Triple mutant tumors demonstrated the presence of large cells (arrow). The SVZ nontumor–tumor boundary is demarcated by the dotted lines; T = tumor, N = nontumor. Scale bars = 100 µm. (C) Quantitative analysis of tumor cellularity between double mutant and triple mutant (mean ± SD, $n = 3$; $^{**}P < 0.01$, Student's *t*-test). (D) Kaplan–Meier survival analysis of double mutant mice ($n = 10$), triple mutant *Creb$^{\Delta}$* mice ($n = 11$), and WT mice (all brains were dissected at 167 days post-tamoxifen).

forced differentiation, suggesting that *Pik3ca^{H1047R}–Pten$^{\Delta}$* mutations stabilize stem cell properties, and, in a clinical setting, these mutations may impart stable, therapy-resistant characteristics with enhanced capacity for tumor recurrence.

Phospho-GSK3β expression was increased in mutant NSPCs, suggesting hyperactivation of the Wnt pathway.[40] Wnt and PI3K signaling are commonly coactivated in stem cells, consistent with enhanced neurosphere-forming capacity of *Pik3ca^{H1047R}–Pten$^{\Delta}$* mutant NSPCs. Wnt signaling is critical for maintaining efficient self-renewal of NSPCs[41,42] and glioma stem cell self-renewal.[43,44] The clinical importance of Wnt signaling in gliomas is highlighted by the correlation of Wnt factors with independent markers of poor prognosis.[45]

We and others have shown that the kinase-inducible transcription factor CREB and its activated form, pCREB, are expressed in GBM[14,46] and that CREB has a role in glioma cell proliferation.[14] Aside from the expected upregulation of the PI3K pathway factors in *Pik3ca^{H1047R}–Pten$^{\Delta}$* tumors, the MAPK

pathway was also upregulated, consistent with observations that CREB sits at a transcriptional convergence point of the PI3K and MAPK pathways.[14] CREB deletion in *Pik3ca*^{H1047R}–*Pten*$^{\Delta}$ NSPCs showed that mutant *Pik3ca*^{H1047R}–*Pten*$^{\Delta}$–*Creb*$^{\Delta}$ mice were symptom free for a longer time compared with double mutant *Pik3ca*^{H1047R}–*Pten*$^{\Delta}$ mice. CREB loss resulted in reduced tumor cellularity and larger tumor cells, suggestive of a less malignant, giant-cell GBM, which has a better prognosis compared with classical GBM.[47] Moreover, no invasion into white matter tracts was observed in triple mutant brains. This is the first in vivo data demonstrating that CREB deletion in tumor cells suppresses tumor growth, consistent with studies correlating aberrant CREB expression and activation with poor prognosis in many neoplasms, including lung[48] and breast.[49]

Overall, our data lead us to propose a model in which the PI3K pathway is critical and sufficient for reprogramming normal NSPCs into tumor-initiating cells. Additionally, we show that mutation of the catalytic PI3K subunit, p110α, leads to transformation of NSPCs into low-grade oligodendroglial-like tumors but that simultaneous PTEN loss enhances oncogenesis, resulting in fast, aggressive tumor growth. As the PI3K mutant tumor cells mature, a CREB-dependent transcriptome is activated, which supports tumor growth. MAPK signaling is also coactivated, further enhancing CREB activation. The Wnt pathway is also hyperactivated and contributes to promoting NSPC self-renewal. Deleting CREB in tumor cells alters the tumor cell phenotype, slows tumor cell growth, and extends symptom-free survival. Recently developed experimental compounds which target CREB can inhibit tumor cell proliferation in vitro and in vivo.[50] Co-targeting archetypal oncogenic pathways, including PI3K, MAPK, and Wnt, as well as transcription factors such as CREB, may prove to be an effective therapeutic approach for difficult to treat cancers, including HGGs.

Supplementary Material

Supplementary material is available at *Neuro-Oncology* online.

Funding

This work was supported by the Department of Pathology, CASS Foundation grant 6236. W.A.P. was supported in part by project grant 1080491 from the National Health and Medical Research Council (NHMRC) of Australia.

Acknowledgments

We thank Rob Ramsay, Andrew Allen, Daniel Gough, Jason Cain, and Ryan Hutchinson for helpful scientific discussions; Tina Isaakidis for proofreading, Sarah Louise Taverner for dedicated animal care and monitoring throughout this project, as well as Teresa Drever, Jessica Sturrock, Michelle Williams, and Marica Kesar for running and managing an excellent animal facility; Daniel Blashki and Vanta Jameson for flow cytometry assistance.

Conflict of interest statement. The authors confirm that they have no conflict of interest regarding the content of the present article.

References

1. Holland EC, Hively WP, DePinho RA, Varmus HE. A constitutively active epidermal growth factor receptor cooperates with disruption of G1 cell-cycle arrest pathways to induce glioma-like lesions in mice. *Genes Dev*. 1998;12(23):3675–3685.
2. Holland EC, Celestino J, Dai C, Schaefer L, Sawaya RE, Fuller GN. Combined activation of Ras and Akt in neural progenitors induces glioblastoma formation in mice. *Nat Genet*. 2000;25(1):55–57.
3. Alcantara Llaguno S, Chen J, Kwon CH, et al. Malignant astrocytomas originate from neural stem/progenitor cells in a somatic tumor suppressor mouse model. *Cancer Cell*. 2009;15(1):45–56.
4. Chow LM, Endersby R, Zhu X, et al. Cooperativity within and among Pten, p53, and Rb pathways induces high-grade astrocytoma in adult brain. *Cancer Cell*. 2011;19(3):305–316.
5. Ozawa T, Riester M, Cheng YK, et al. Most human non-GCIMP glioblastoma subtypes evolve from a common proneural-like precursor glioma. *Cancer Cell*. 2014;26(2):288–300.
6. Alcantara Llaguno SR, Wang Z, Sun D, et al. Adult lineage-restricted CNS progenitors specify distinct glioblastoma subtypes. *Cancer Cell*. 2015;28(4):429–440.
7. Danks RA, Orian JM, Gonzales MF, et al. Transformation of astrocytes in transgenic mice expressing SV40 T antigen under the transcriptional control of the glial fibrillary acidic protein promoter. *Cancer Res*. 1995;55(19):4302–4310.
8. Friedmann-Morvinski D, Bushong EA, Ke E, et al. Dedifferentiation of neurons and astrocytes by oncogenes can induce gliomas in mice. *Science*. 2012;338(6110):1080–1084.
9. Liu C, Sage JC, Miller MR, et al. Mosaic analysis with double markers reveals tumor cell of origin in glioma. *Cell*. 2011;146(2):209–221.
10. Jacques TS, Swales A, Brzozowski MJ, et al. Combinations of genetic mutations in the adult neural stem cell compartment determine brain tumour phenotypes. *EMBO J*. 2010;29(1):222–235.
11. Robinson JP, VanBrocklin MW, Guilbeault AR, Signorelli DL, Brandner S, Holmen SL. Activated BRAF induces gliomas in mice when combined with Ink4a/Arf loss or Akt activation. *Oncogene*. 2010;29(3):335–344.
12. Zhu Z, Khan MA, Weiler M, et al. Targeting self-renewal in high-grade brain tumors leads to loss of brain tumor stem cells and prolonged survival. *Cell Stem Cell*. 2014;15(2):185–198.
13. Peltier J, O'Neill A, Schaffer DV. PI3K/Akt and CREB regulate adult neural hippocampal progenitor proliferation and differentiation. *Dev Neurobiol*. 2007;67(10):1348–1361.
14. Daniel P, Filiz G, Brown DV, et al. Selective CREB-dependent cyclin expression mediated by the PI3K and MAPK pathways supports glioma cell proliferation. *Oncogenesis*. 2014;3:e108.
15. Padala RR, Karnawat R, Viswanathan SB, Thakkar AV, Das AB. Cancerous perturbations within the ERK, PI3K/Akt, and Wnt/β-catenin signaling network constitutively activate inter-pathway positive feedback loops. *Mol Biosyst*. 2017;13(5):830–840.
16. Rheinbay E, Suvà ML, Gillespie SM, et al. An aberrant transcription factor network essential for Wnt signaling and stem cell maintenance in glioblastoma. *Cell Rep*. 2013;3(5):1567–1579.

17. Kita D, Yonekawa Y, Weller M, Ohgaki H. PIK3CA alterations in primary (de novo) and secondary glioblastomas. *Acta Neuropathol*. 2007;113(3):295–302.
18. Tamborero D, Gonzalez-Perez A, Perez-Llamas C, et al. Comprehensive identification of mutational cancer driver genes across 12 tumor types. *Sci Rep*. 2013;3:2650.
19. Broderick DK, Di C, Parrett TJ, et al. Mutations of PIK3CA in anaplastic oligodendrogliomas, high-grade astrocytomas, and medulloblastomas. *Cancer Res*. 2004;64(15):5048–5050.
20. Chalhoub N, Baker SJ. PTEN and the PI3-kinase pathway in cancer. *Annu Rev Pathol*. 2009;4:127–150.
21. Di Cristofano A, Pandolfi PP. The multiple roles of PTEN in tumor suppression. *Cell*. 2000;100(4):387–390.
22. Gregorian C, Nakashima J, Le Belle J, et al. Pten deletion in adult neural stem/progenitor cells enhances constitutive neurogenesis. *J Neurosci*. 2009;29(6):1874–1886.
23. Groszer M, Erickson R, Scripture-Adams DD, et al. Negative regulation of neural stem/progenitor cell proliferation by the Pten tumor suppressor gene in vivo. *Science*. 2001;294(5549):2186–2189.
24. Kinross KM, Montgomery KG, Kleinschmidt M, et al. An activating Pik3ca mutation coupled with Pten loss is sufficient to initiate ovarian tumorigenesis in mice. *J Clin Invest*. 2012;122(2):553–557.
25. Imayoshi I, Ohtsuka T, Metzger D, Chambon P, Kageyama R. Temporal regulation of Cre recombinase activity in neural stem cells. *Genesis*. 2006;44(5):233–238.
26. Mantamadiotis T, Lemberger T, Bleckmann SC, et al. Disruption of CREB function in brain leads to neurodegeneration. *Nat Genet*. 2002;31(1):47–54.
27. Casanova E, Fehsenfeld S, Lemberger T, Shimshek DR, Sprengel R, Mantamadiotis T. ER-based double iCre fusion protein allows partial recombination in forebrain. *Genesis*. 2002;34(3):208–214.
28. Hu Y, Smyth GK. ELDA: extreme limiting dilution analysis for comparing depleted and enriched populations in stem cell and other assays. *J Immunol Methods*. 2009;347(1–2):70–78.
29. Liang H, Hippenmeyer S, Ghashghaei HT. A Nestin-cre transgenic mouse is insufficient for recombination in early embryonic neural progenitors. *Biol Open*. 2012;1(12):1200–1203.
30. Kinross KM, Montgomery KG, Mangiafico SP, et al. Ubiquitous expression of the Pik3caH1047R mutation promotes hypoglycemia, hypoinsulinemia, and organomegaly. *FASEB J*. 2015;29(4):1426–1434.
31. Memmel S, Sukhorukov VL, Höring M, et al. Cell surface area and membrane folding in glioblastoma cell lines differing in PTEN and p53 status. *PLoS One*. 2014;9(1):e87052.
32. Dworkin S, Malaterre J, Hollande F, Darcy PK, Ramsay RG, Mantamadiotis T. cAMP response element binding protein is required for mouse neural progenitor cell survival and expansion. *Stem Cells*. 2009;27(6):1347–1357.
33. Amiri A, Cho W, Zhou J, et al. Pten deletion in adult hippocampal neural stem/progenitor cells causes cellular abnormalities and alters neurogenesis. *J Neurosci*. 2012;32(17):5880–5890.
34. Hartmann C, Bartels G, Gehlhaar C, Holtkamp N, von Deimling A. PIK3CA mutations in glioblastoma multiforme. *Acta Neuropathol*. 2005;109(6):639–642.
35. Maehama T, Dixon JE. The tumor suppressor, PTEN/MMAC1, dephosphorylates the lipid second messenger, phosphatidylinositol 3,4,5-trisphosphate. *J Biol Chem*. 1998;273(22):13375–13378.
36. Chen H, Mei L, Zhou L, et al. PTEN restoration and PIK3CB knockdown synergistically suppress glioblastoma growth in vitro and in xenografts. *J Neurooncol*. 2011;104(1):155–167.
37. Pridham KJ, Le L, Guo S, et al. PIK3CB/p110beta is a selective survival factor for glioblastoma. *Neuro Oncol*. 2017;20(4):494–505.
38. Kubiatowski T, Jang T, Lachyankar MB, et al. Association of increased phosphatidylinositol 3-kinase signaling with increased invasiveness and gelatinase activity in malignant gliomas. *J Neurosurg*. 2001;95(3):480–488.
39. Wei Y, Jiang Y, Zou F, et al. Activation of PI3K/Akt pathway by CD133-p85 interaction promotes tumorigenic capacity of glioma stem cells. *Proc Natl Acad Sci U S A*. 2013;110(17):6829–6834.
40. McManus EJ, Sakamoto K, Armit LJ, et al. Role that phosphorylation of GSK3 plays in insulin and Wnt signalling defined by knockin analysis. *EMBO J*. 2005;24(8):1571–1583.
41. Kalani MY, Cheshier SH, Cord BJ, et al. Wnt-mediated self-renewal of neural stem/progenitor cells. *Proc Natl Acad Sci U S A*. 2008;105(44):16970–16975.
42. Wexler EM, Paucer A, Kornblum HI, Palmer TD, Plamer TD, Geschwind DH. Endogenous Wnt signaling maintains neural progenitor cell potency. *Stem Cells*. 2009;27(5):1130–1141.
43. Pulvirenti T, Van Der Heijden M, Droms LA, Huse JT, Tabar V, Hall A. Dishevelled 2 signaling promotes self-renewal and tumorigenicity in human gliomas. *Cancer Res*. 2011;71(23):7280–7290.
44. Zhang N, Wei P, Gong A, et al. FoxM1 promotes β-catenin nuclear localization and controls Wnt target-gene expression and glioma tumorigenesis. *Cancer Cell*. 2011;20(4):427–442.
45. Liu C, Tu Y, Sun X, et al. Wnt/beta-catenin pathway in human glioma: expression pattern and clinical/prognostic correlations. *Clin Exp Med*. 2011;11(2):105–112.
46. Barresi V, Mondello S, Branca G, Rajan TS, Vitarelli E, Tuccari G. p-CREB expression in human gliomas: potential use in the differential diagnosis between astrocytoma and oligodendroglioma. *Hum Pathol*. 2015;46(2):231–238.
47. Kozak KR, Moody JS. Giant cell glioblastoma: a glioblastoma subtype with distinct epidemiology and superior prognosis. *Neuro Oncol*. 2009;11(6):833–841.
48. Liu W, Wu Y, Wang L, et al. Protein signature for non-small cell lung cancer prognosis. *Am J Cancer Res*. 2014;4(3):256–269.
49. Chhabra A, Fernando H, Watkins G, Mansel RE, Jiang WG. Expression of transcription factor CREB1 in human breast cancer and its correlation with prognosis. *Oncol Rep*. 2007;18(4):953–958.
50. Xie F, Li BX, Kassenbrock A, et al. Identification of a potent inhibitor of CREB-mediated gene transcription with efficacious in vivo anticancer activity. *J Med Chem*. 2015;58(12):5075–5087.